Engineering 6 (2020) 173–177

Contents lists available at ScienceDirect

Engineering

journal homepage: www.elsevier.com/locate/eng

Research
Rare Earth Permanent Magnets—Article

Efficient Nanostructuring of Isotropic Gas-Atomized MnAl Powder by Rapid Milling (30 s)

J. Rial, E.M. Palmero, A. Bollero *

Division of Permanent Magnets and Applications, IMDEA Nanoscience, Campus Universidad Autónoma de Madrid, Madrid 28049, Spain

ARTICLE INFO

Article history:
Received 31 July 2018
Revised 11 March 2019
Accepted 12 March 2019
Available online 15 June 2019

Keywords:
Permanent magnets (PMs)
Nanostructuring
Phase transformation
MnAl
Gas atomization
Ball milling

ABSTRACT

An unprecedentedly short milling time of 30 s was applied to gas-atomized MnAl powder in order to develop permanent magnet properties and, in particular, coercivity. It is shown that such a short processing time followed by annealing results in efficient nanostructuring and controlled phase transformation. The defects resulting from the microstrain induced during milling, together with the creation of the β-phase during post-annealing, act as pinning centers resulting in an enhanced coercivity. This study shows the importance of finding a balance between the formation of the ferromagnetic τ-MnAl phase and the β-phase in order to establish a compromise between magnetization and coercivity. A coercivity as high as 4.2 kOe (1 Oe = 79.6 A·m^{-1}) was obtained after milling (30 s) and annealing, which is comparable to values previously reported in the literature for milling times exceeding 20 h. This reduction of the post-annealing temperature by 75 °C for the as-milled powder and a 2.5-fold increase in coercivity, while maintaining practically unchanged the remanence of the annealed gas-atomized material, opens a new path for the synthesis of isotropic MnAl-based powder.

1. Introduction

Numerous present and emerging technologies require the use of permanent magnets (PMs), resulting in an increasing yearly need for rare-earth (RE) elements as constituents of the strongest (NdFeB- and SmCo-based) technological PMs [1,2]. Economic and environmental considerations have attracted the interest of research groups and industry in the search for RE-free PM alternatives [3], which should result in diversification of the PM sector according to the requirements of the final application. Ferrites are low-cost PMs with widely abundant constituent elements; however, the reduced maximum energy product, $(BH)_{max}$, of about 5 megagauss-oersteds (MGOe, 1 MGOe = 7.958 kJ·m^{-3}) is a limiting factor for applications requiring a high magnetic performance.

MnAl is a promising RE-free PM candidate with a high uniaxial magnetocrystalline anisotropy ($K \approx 1.5 \times 10^6$ J·m^{-3}) and a theoretical $(BH)_{max}$ of 12 MGOe [4,5]. These values, in combination with a low density (5.2 g·cm^{-3}) in comparison with that of $Nd_2Fe_{14}B$ (7.4 g·cm^{-3}), would result in a high-energy product per unit weight—that is, in high-performance light magnets. MnAl has only one ferromagnetic phase, the τ-MnAl phase. This is a metastable phase that can be obtained by annealing from the most stable ε-phase. The annealing process develops the ferromagnetic τ-phase and, therefore, the magnetization of the sample. However, the coercivity (H_c) of the annealed powder is typically below 2 kOe (1 Oe = 79.6 A·m^{-1}) [6–8]. The ball-milling process is a suitable technique to increase the H_c of the material through controlled nanostructuring [7,9–11]. The literature reports that a typical milling time of several hours is necessary to develop H_c [7–12]; however, it has recently been demonstrated that milling times as short as a few minutes can lead to comparable H_c [13,14]. In this work, an extremely short milling time of 30 s, which is sufficient for nanostructuring without inducing amorphization, was applied to study the evolution of the magnetic properties of gas-atomized MnAl powder.

2. Experimental details

Gas-atomized powder with a composition of $Mn_{54}Al_{46}$ (±0.4 at%) was used as the starting material. Details about preparation and composition have been published elsewhere [8]. The gas-atomized powder showed approximately spherical particles with a diameter less than 10 μm (Fig. 1). The gas-atomized powder

* Corresponding author.
E-mail address: alberto.bollero@imdea.org (A. Bollero).

https://doi.org/10.1016/j.eng.2019.03.013

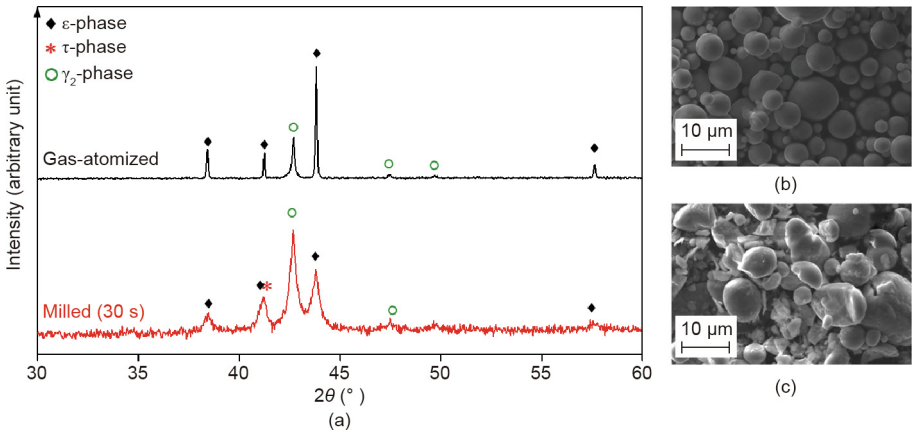

Fig. 1. (a) X-ray diffraction (XRD) patterns of the gas-atomized and the as-milled (30 s) powders. Scanning electron microscope (SEM) images of the (b) gas-atomized and (c) as-milled powders.

was surfactant-assisted (oleic acid) ball milled for 30 s, in order to reduce possible oxidation and avoid welding. The ball-milling process was performed with tungsten carbide vials and balls, with a typical rotation speed of 900 r·min^{-1}. The powder-to-oleic acid ratio was 5:1, and the ball-to-powder mass was 40:1. The loading and sealing of the vials were performed in an argon (Ar)-controlled atmosphere glove box to prevent oxidation. The particles morphology was determined using a Zeiss-EVO scanning electron microscope (SEM). A differential scanning calorimeter (DSC)—namely, TA Instruments model SDT Q600—was used to determine the crystallographic transition temperatures. MnAl powders were annealed under a nitrogen (N_2) flow of 100 mL·min^{-1} up to 700 °C, using a temperature ramp of 10 K·min^{-1}. X-ray diffraction (XRD) measurements were carried out using a Panalytical X'Pert PRO theta/2theta diffractometer with Cu-Kα radiation (λ = 0.1541 nm). The crystallite size and microstrain were determined by the Scherrer method. Details on the quantitative phase analysis of milled and post-annealed powders are provided elsewhere [13]. As-atomized and milled powders were annealed under N_2 flow with a ramp rate of 10 °C·min^{-1} at temperatures (T_{anneal}) of 340–450 °C for 10 min. Room-temperature hysteresis loops were measured using a Lakeshore 7400 series vibrating sample magnetometer (VSM) with a maximum applied field of 20 kOe. These measurements allowed for the determination of the magnetization measured at a maximum applied field of 20 kOe (M_{20kOe}), the remanence (M_r), and the H_c.

3. Results and discussion

Fig. 1(a) shows the XRD patterns measured for the gas-atomized powder in the as-prepared state and after milling for 30 s. The gas-atomized powder consisted of the ε-phase with a minor content of the γ_2-phase. The crystallite size determined from the XRD pattern for the ε-phase was 110 nm. Milling for 30 s was sufficient to produce breakage of the particles, but there was no significant change in the average particle size in comparison with that of the starting powder (Fig. 1). The mean crystallite size was clearly reduced, as may be directly inferred from the broader diffraction peaks measured after milling (Fig. 1(a)). In addition, and not reported to date by other milling methods, formation of the τ-MnAl phase was already observed in the as-milled state—that is, prior to annealing the powder—due to the reported high impact energy exerted during the process when milling with a high-density milling media (tungsten carbide) [14]. It is precisely the combination of a high impact energy (inducing microstrain) and the application of an extremely short milling time (avoiding the high temperature achieved during long milling times—i.e., undesired relaxation effects) that probably eases the beginning of the ε-to-τ phase transformation through a displacive shear mechanism already occurring in the as-milled state. Fig. 2 shows the DSC heating curve measured for the starting gas-atomized powder and for the powder milled for 30 s. The measured exothermic peak corresponds to the ε-to-τ phase transformation [13], with a maximum at 440 and 390 °C for the gas-atomized powder and as-milled powder, respectively. Thus, milling for such a short time resulted in a decreased transformation temperature, which is of interest in view of possible powder manufacturing. This decreased temperature was a direct consequence of the microstructural refinement produced during the milling process in combination with the defects introduced in the particles, which decreased the energy barrier to produce the τ-MnAl phase [14].

Both samples (i.e., the gas-atomized and as-milled powders) were annealed in the temperature range of 340–450 °C to check the evolution of the magnetic properties with T_{anneal} (Fig. 3). No morphological transformation was observed in the samples after annealing, so the same particle size was maintained.

The magnetization values M_r and M_{20kOe} showed the same tendency with increasing T_{anneal}, as shown in Fig. 3(a). However, a remarkable difference in the T_{anneal} needed to achieve maximum magnetization values was observed, with 75 °C less needed for the as-milled powder (T_{anneal} = 375 °C) to achieve the maximum

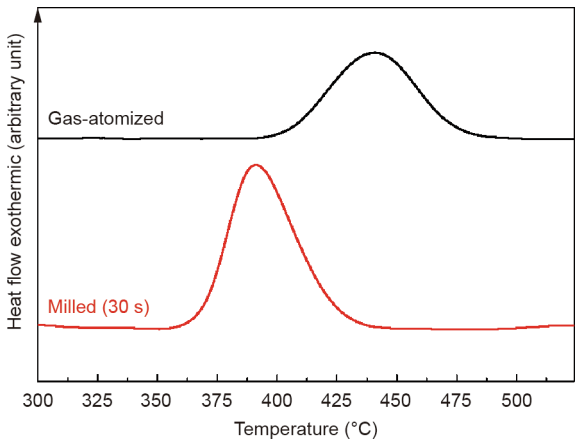

Fig. 2. DSC curves of the gas-atomized and as-milled (30 s) powders.

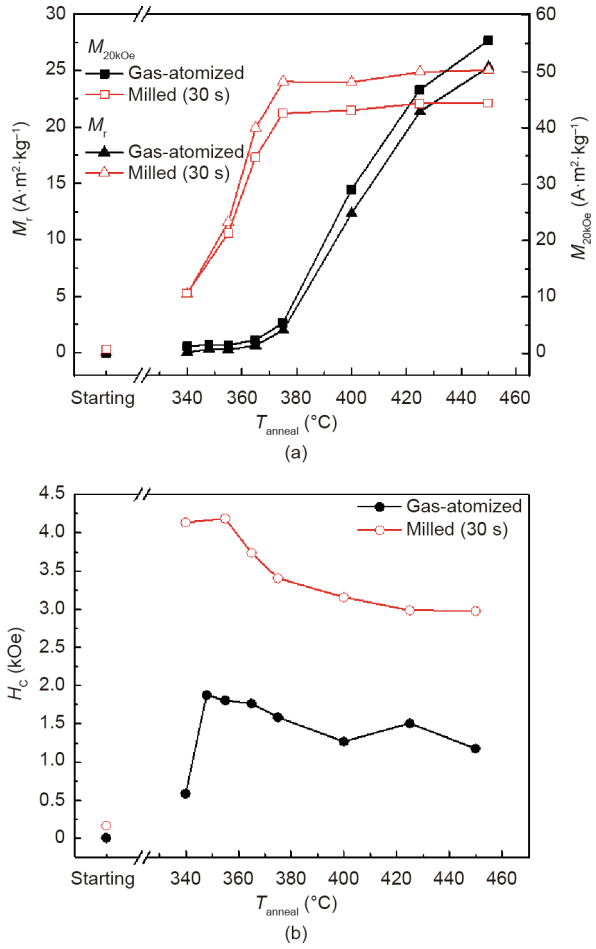

Fig. 3. Evolution of the magnetic properties for gas-atomized and as-milled (30 s) powders: (a) M_r and M_{20kOe}; (b) H_c.

value, in comparison with the gas-atomized powder (T_{anneal} = 450 °C). This finding is of technological significance when considering the potential industrial implementation of the process. This fact is clearly illustrated in Fig. 4, where selected hysteresis loops are displayed for the gas-atomized and as-milled powders after annealing at 365 and 450 °C (Figs. 4(a) and (b), respectively). As may be observed, T_{anneal} = 365 °C was insufficient to develop adequate PM properties in the gas-atomized powder, whereas T_{anneal} = 450 °C guaranteed full development of the magnetic properties. Although this temperature of 450 °C was not the optimum one to be applied to the as-milled powder, it is worth remarking that the M_r remained approximately the same while the H_c was 2.5 times higher for the milled and annealed powder, thereby proving the efficiency of this method in nanostructuring and improving the magnetic properties.

The evolution of the magnetization with annealing temperature can be understood by looking at the phase evolution of the gas-atomized and as-milled powders with T_{anneal} (Fig. 5). The gas-atomized powder required T_{anneal} > 365 °C to initiate the formation of the τ-phase. At 400 °C, the ε-to-τ transformation was incomplete; thus, both phases were co-existing. The ε-to-τ transformation was only concluded at 450 °C, when the τ-phase was observed together with a minor content of the β-phase. In comparison, milling for 30 s was sufficient to generate the τ-phase in the as-milled state—that is, with no need for a post-annealing treatment. Further annealing was required to enhance the τ-phase content and, consequently, the magnetization (Fig. 3(a)). It is worth noting that while annealing at 365 °C did not result in appreciable nucleation of the τ-phase in the XRD pattern of the starting

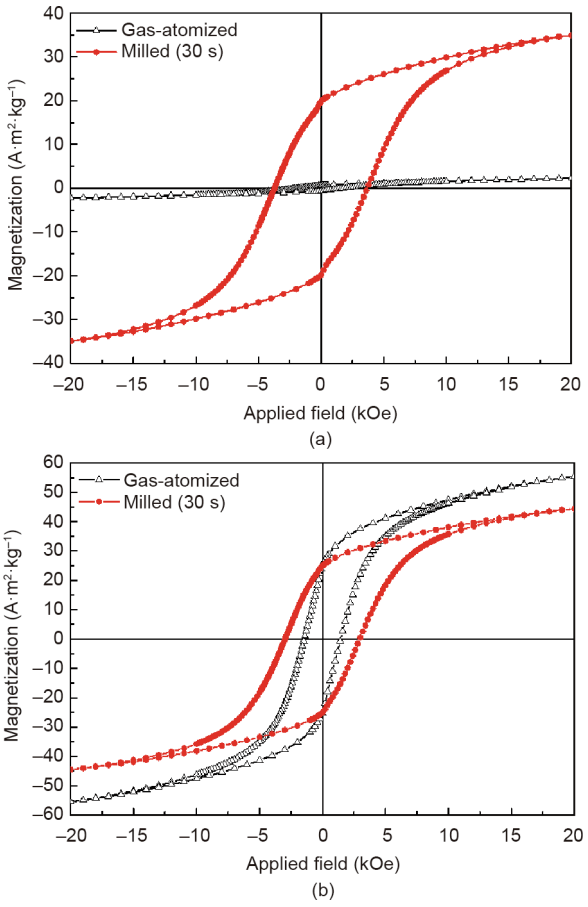

Fig. 4. Room-temperature hysteresis loops measured for the gas-atomized and as-milled powders after annealing at (a) 365 °C and (b) 450 °C.

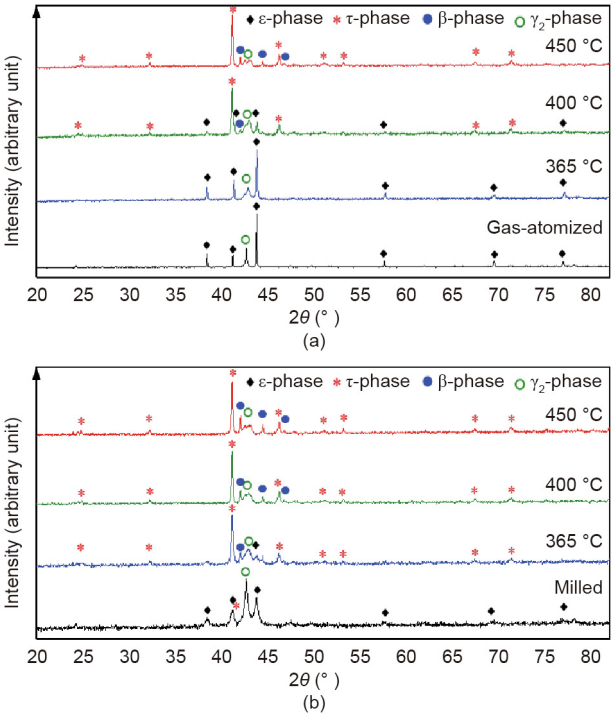

Fig. 5. XRD patterns of the (a) gas-atomized and (b) as-milled powders, in the as-prepared state and after annealing at 365, 400, and 450 °C.

Table 1
Evolution of the β/τ ratio, mean crystallite size, mean strain induced during milling, and H_c with the annealing temperature for the as-atomized and milled (30 s) powder.

Sample	Temperature (°C)	β/τ ratio	Mean crystallite size (nm)	Mean strain (%)	H_c (kOe)
Gas-atomized	365	–	–	–	1.8
	400	0.11	53	0.19	1.3
	450	0.18	63	0.16	1.2
Milled (30 s)	365	0.24	43	0.23	3.7
	400	0.25	54	0.19	3.2
	450	0.36	57	0.18	3.0

powder, the same temperature applied to the powder milled for 30 s promoted almost the full transformation of the ε-phase into the τ-MnAl phase; at 400 °C, there was nothing reminiscent of the diffraction peaks of the ε-phase. The significantly decreased temperature needed for the ε-to-τ phase transformation in the case of the as-milled powder is in good agreement with the DSC results (Fig. 2). Consequently, the evolution of the magnetization values (M_r and M_{20kOe}) with T_{anneal} is fully consistent with the evolution of the ferromagnetic τ-phase content. The lower magnetization values measured for the milled and annealed powder are a direct consequence of the higher β/τ fraction content (Table 1). It is worth remarking that enhanced magnetization values might be obtained in both the gas-atomized and the milled and annealed powder by starting from an ε single-phase gas-atomized powder (i.e., by avoiding the presence of secondary phases in the starting material).

Additional factors should be taken into account in order to understand the behavior of the H_c with increasing T_{anneal} (Fig. 3(b)). Previous studies [7,14] have shown that the β/τ fraction content and the strain induced during milling are the main factors determining H_c in MnAl powder. Table 1 summarizes these values for the samples under study after annealing at different temperatures. Annealing of the gas-atomized and the as-milled powders resulted in an increased mean crystallite size with increasing T_{anneal}, which remained below 65 nm. For the same T_{anneal}, the crystallite size was smaller in all cases for the milled and annealed powder.

Milling of the gas-atomized powder resulted in a decreased mean crystallite size in combination with the microstrain induced during the milling process. The novelty of the approach followed in this study, in comparison with previous results reported by the same authors on milling times ranging from 90 to 270 s [14], is that those times were sufficient to begin amorphization of the MnAl. It was proven that post-annealing of the as-milled powder favors recrystallization into the β-phase, which is beneficial to some extent (provided an adequate β/τ ratio) to increase H_c but detrimental to the magnetization by reducing the overall τ-phase content. In the present study, milling for 30 s resulted in microstructural refinement without initiating amorphization of the powder.

The maximum H_c of 1.8 and 4.2 kOe obtained for the annealed gas-atomized powder and as-milled powder, respectively, was a consequence of the combined effect of the reduced mean crystallite size, induced strain, and enhanced β/τ ratio. The formation of defects during milling and the creation of the β-phase played an important role as pinning centers in the magnetization reversal mechanism by increasing H_c. Annealing the powder resulted in grain growth and relaxation effects (Table 1), thus reducing the H_c with increasing T_{anneal} (Fig. 3(b)). This combination of gas atomization and flash milling (30 s) offers a new route for the fabrication of isotropic nanocrystalline MnAl powder, with potential applications in emerging technologies such as 3D printing [15].

4. Conclusions

The milling of gas-atomized MnAl powder for an unprecedentedly short time of 30 s made H_c development possible, with a maximum value of 4.2 kOe after post-annealing in comparison with 1.8 kOe obtained for the starting material. This result was a consequence of nanostructuring without the initiation of amorphization, and a control on the β/τ ratio during the process. A short milling time of 30 s avoids the high temperature typically achieved when milling for a long time, and thus avoids undesired relaxation and phase-transformation effects. The annealing temperature required to achieve the best combination of magnetic properties in the as-milled powder was 75 °C lower than that of the gas-atomized powder. The reduced ε-to-τ phase-transformation temperature and the possibility of developing H_c about 2.5 times greater than those of the gas-atomized powder while maintaining M_r make this route a promising one for the fabrication of nanocrystalline MnAl powder.

Acknowledgements

Gas-atomized powder was provided by Prof. Ian Baker (Dartmouth College) and Prof. Laura H. Lewis (Northeastern University, Boston) (Energy (ARPA-E), REACT DE-AR0000188). The authors acknowledge financial support from MINECO through NEXMAG (M-era.Net, PCIN-2015-126) and 3D-MAGNETOH (MAT2017-89960-R) projects; and from the Regional Government of Madrid through the NANOMAGCOST (P2018/NMT-4321) project. IMDEA Nanociencia is supported by the "Severo Ochoa" Programme for Centres of Excellence in R&D, MINECO (SEV-2016-0686).

Compliance with ethics guidelines

J. Rial, E.M. Palmero, and A. Bollero declare that they have no conflict of interest or financial conflicts to disclose.

References

[1] Coey JMD. Hard magnetic materials: a perspective. IEEE Trans Magn 2011;47(12):4671–81.
[2] Lewis LH, Jiménez-Villacorta F. Perspectives on permanent magnetic materials for energy conversion and power generation. Metall Mater Trans A 2013;44(S1):2–20.
[3] Gutfleisch O, Willard MA, Brück E, Chen CH, Sankar SG, Liu JP. Magnetic materials and devices for the 21st century: stronger, lighter, and more energy efficient. Adv Mater 2011;23(7):821–42.
[4] Koch AJJ, Hokkeling P, Steeg MG, de Vos KJ. New material for permanent magnets on a base of Mn and Al. J Appl Phys 1960;31(5):S75–7.
[5] Kōno H. On the ferromagnetic phase in manganese–aluminum system. J Phys Soc Jpn 1958;13(12):1444–51.
[6] Jiménez-Villacorta F, Marion JL, Oldham JT, Daniil M, Willard MA, Lewis LH. Magnetism-structure correlations during the ε→τ transformation in rapidly-solidified MnAl nanostructured alloys. Metals 2014;4(1):8–19.
[7] Zeng Q, Baker I, Cui JB, Yan ZC. Structural and magnetic properties of nanostructured Mn–Al–C magnetic materials. J Magn Magn Mater 2007;308(2):214–26.
[8] Chatuverdi A, Yaqub R, Baker I. Microstructure and magnetic properties of bulk nanocrystalline MnAl. Metals 2014;4(1):20–7.
[9] Marshall LG, McDonald IJ, Lewis LH. Quantification of the strain-induced promotion of τ-MnAl via cryogenic milling. J Magn Magn Mater 2016;404:215–20.
[10] Jian H, Skokov KP, Gutfleisch O. Microstructure and magnetic properties of Mn–A1–C alloy powders prepared by ball milling. J Alloys Compd 2015;622:524–8.

[11] Bittner F, Freudenberger J, Schultz L, Woodcock TG. The impact of dislocations on coercivity in $L1_0$-MnAl. J Alloys Compd 2017;704:528–36.
[12] Lee JG, Wang XL, Zhang ZD, Choi CJ. Effect of mechanical milling and heat treatment on the structure and magnetic properties of gas atomized Mn–Al alloy powders. Thin Solid Films 2011;519(23):8312–6.
[13] Law JY, Rial J, Villanueva M, López N, Camarero J, Marshall LG, et al. Study of phases evolution in high-coercive MnAl powders obtained through short milling time of gas-atomized particles. J Alloys Compd 2017;712:373–8.
[14] Rial J, Švec P, Palmero EM, Camarero J, Švec P Sr, Bollero A. Severe tuning of permanent magnet properties in gas-atomized MnAl powder by controlled nanostructuring and phase transformation. Acta Mater 2018;157:42–52.
[15] Palmero EM, Rial J, de Vicente J, Camarero J, Skårman B, Vidarsson H, et al. Development of permanent magnet MnAlC/polymer composites and flexible filament for bonding and 3D-printing technologies. Sci Technol Adv Mater 2018;19(1):465–73.